

DR. ALBERTO JAVIER RAMOS (Orcid ID : 0000-0003-4009-6337)

Article type : Original Article

## **G5G2.5 core-shell tecto-dendrimer specifically targets reactive glia in brain ischemia**

Veronica Murta<sup>1-2</sup>; Priscila Schilrreff<sup>3</sup>, Gerardo Rosciszewski<sup>1-2</sup>, Maria Jose Morrilla<sup>3</sup>, Alberto Javier Ramos<sup>1-2\*</sup>

<sup>1</sup>Universidad de Buenos Aires, Facultad de Medicina, Departamento de Histología, Embriología, Biología Celular y Genética, Buenos Aires, Argentina

<sup>2</sup>Laboratorio de Neuropatología Molecular, Instituto de Biología Celular y Neurociencia “Prof. E. De Robertis” IBCN UBA-CONICET, Buenos Aires, Argentina.

<sup>3</sup>Programa de Nanomedicinas, Departamento de Ciencia y Tecnología, Universidad Nacional de Quilmes, Bernal, Argentina.

**\*Corresponding author:**

Dr. Alberto Javier Ramos

Laboratorio de Neuropatología Molecular,

Instituto de Biología Celular y Neurociencia “Prof. E. De Robertis” UBA-CONICET

Facultad de Medicina

Universidad de Buenos Aires

Calle Paraguay 2155 3er piso

(1121) Ciudad de Buenos Aires

Argentina.

This article has been accepted for publication and undergone full peer review but has not been through the copyediting, typesetting, pagination and proofreading process, which may lead to differences between this version and the Version of Record. Please cite this article as doi: 10.1111/jnc.14286

This article is protected by copyright. All rights reserved.

E-mail: jramos@fmed.uba.ar

Tel/Fax: 54-11-5950-9626

Running title: G5G2.5 tecto-dendrimer targets reactive glia

Key Words: astrocyte; neuroinflammation; nanoparticle; stroke

Funding: Supported by grants of CONICET PIP 387 and 479 (to AJR), ANPCYT PICT2012-1424 and PICT2015-1451 (to AJR), UBACYT (to AJR)

#### **Abbreviations**

BBB: blood-brain barrier

CD: cortical devascularization

CNS: central nervous system

DIV: days in vitro

DPL: days post ischemic lesion

FBS: Fetal bovine serum

FITC: fluorescein isothiocyanate isomer I

GFAP: Glial fibrillary acidic protein

h: hours

HBSS: Hank's Balanced Salt Solution

LPS: Lipopolysaccharide

MTT: 3-(4,5-dimethylthiazole-2-yl)-2,5-diphenyltetrazolium bromide)

OGD: Oxygen and glucose deprivation

PAMAM: polyamidoamine

PBS: phosphate-buffered saline

## Abstract

Secondary neuronal death is a serious stroke complication. That process is facilitated by the conversion of glial cells to the reactive proinflammatory phenotype that induces neurodegeneration. Therefore, regulation of glial activation is a compelling strategy to reduce brain damage after stroke. However, drugs have difficulties to access the central nervous system (CNS), and to specifically target glial cells. In the present work we explored the use core-shell polyamidoamine tecto-dendrimer (G5G2.5 PAMAM) and studied its ability to target distinct populations of stroke-activated glial cells. We found that G5G2.5 tecto-dendrimer is actively engulfed by primary glial cells in a time- and dose-dependent manner showing high cellular selectivity and lysosomal localization. In addition, oxygen-glucose deprivation or lipopolysaccharides (LPS) exposure *in vitro* and brain ischemia *in vivo* increase glial G5G2.5 uptake; not being incorporated by neurons or other cell types. We conclude that G5G2.5 tecto-dendrimer is a highly suitable carrier for targeted drug delivery to reactive glial cells *in vitro* and *in vivo* after brain ischemia.

## INTRODUCTION

Stroke, brain attack or brain ischemia is a severe pathological state, that can have devastating consequences for patients. The available therapies are limited to the recanalization of the occluded vessel, a strategy with serious intrinsic risks that requires rapid access to tertiary care healthcare services (Levine *et al.* 2013, Grotta & Hacke 2015).

Following brain ischemia, astroglial and microglial cells become reactive and the cell crosstalk with the innate immune system results in a widespread neuroinflammation that increases secondary neuronal death (Burda & Sofroniew 2014, Liddelow *et al.* 2017). Reactive astrocytes undergo a complex biological process that includes the upregulation of a plethora of genes. In spite that some genes seem to contribute to neuronal survival, others are closely related to proinflammatory pathways that facilitate neurodegeneration and glial scar formation (Zamanian *et al.* 2012, Anderson *et al.* 2014, Burda & Sofroniew 2014, Villarreal *et al.* 2014, Wanner *et al.* 2013, LeComte *et al.* 2015). Microglial cells, on the other hand, become activated by the primary

cell death in the ischemic core and they may suffer polarization to the opposite phenotypes known as the proinflammatory-neurodegenerative M1 or the anti-inflammatory-neuroregenerative M2 profile (reviewed in Huang & Feng 2013)).

The prevailing hypothesis is that controlling glial conversion to the proinflammatory-neurodegenerative phenotypes will dramatically reduce neuroinflammation and will facilitate neuronal survival after stroke, thus reducing patient morbidity and mortality. The pharmacological approach to that end is hindered by the fact that drug access to the central nervous system (CNS) is strictly limited by the presence of the blood-brain barrier (BBB). In addition, most drugs have low cellular selectivity, which seriously precludes their use due to side effects on other cell types.

The nanometer-scale dendrimer-based platforms emerged as promising carriers for different types of drugs due to their capacity to carry different loads, the possibility of chemically modifying their structure and chemically engineering the structure of the carrier (see revision in Kannan *et al.* 2014). Specifically, polyamidoamine (PAMAM) dendrimers stand out as promising targeted delivery nanodevices with potential use in CNS-targeted therapies (Nance *et al.* 2015, Lesniak *et al.* 2013, Kannan *et al.* 2012, Guo *et al.* 2016, Cerqueira *et al.* 2012, Albertazzi *et al.* 2013). Both native hydroxyl-modified generation 4 PAMAM dendrimers (G4-OH) (Nance *et al.* 2015, Lesniak *et al.* 2013, Kannan *et al.* 2012) and other chemically-modified dendrimers (Guo *et al.* 2016, Cerqueira *et al.* 2012, 2013, Albertazzi *et al.* 2013) have been shown to successfully reach the CNS.

The increase in dendrimer generation during synthesis, yielding larger structures that carry larger number of active molecules has shown that, beyond G5 generation, the de Gennes dense-packing phenomenon reduces good monodispersity and precludes ideal dendritic construction leading to a crowding of functional groups in the dendrimer surface (Lothian-Tomalia *et al.* 1997). In this context, the core-shell tecto-dendrimers, which consist of a dendrimer core surrounded by a shell of lower-radii dendrimers, would provide additional loading capacity as drug carriers, yet preserving the well-organized dendrimer structure (Uppuluri *et al.* 2000, Schilrreff *et al.* 2012).

Using the core-shell tecto-dendrimers obtained by conjugating G5 dendrimers as core with G2.5 as shell surface, as previously described (Schilrreff *et al.* 2012), we here explored the tecto-dendrimer ability to specifically reach reactive glia *in vitro* and *in vivo* after brain ischemia, a pharmacological strategy that would make G5G2.5 suitable for glial-targeted therapy.

## METHODS

**Materials.** Cell culture reagents and LysoTracker Red (cat# L7528) were obtained from Invitrogen Life Technologies (RRID:SCR\_008817, Carlsbad, CA, USA). Fetal bovine serum (FBS) was purchased from Natocor (Córdoba, Argentina). Poly-L-lysine (cat# P1399), DAPI (4',6-diamidino-2-phenylindole) (cat# D9542), Ethylenediamine PAMAM G5, G2.5, and G6.5 dendrimers (cat# 536709; 412414 and 536792 respectively), LiCl (cat# L9650), 1-(3-dimethylaminopropyl)-3-ethylcarbodiimide hydrochloride (EDC) (cat# E7750), fluorescein isothiocyanate isomer I (FITC) (cat# F7250), Lipopolysaccharides (LPS) from *Escherichia coli* O26:B6 (cat# L8274), 3-(4,5-dimethylthiazole-2-yl)-2,5-diphenyltetrazolium bromide) (MTT) (cat# M2128), high-retention cellulose dialysis tubing, Sephadex G-100 (cat# S6147) and G-25 (cat# S5772) and other chemicals were purchased from Sigma-Aldrich (RRID:SCR\_008988; MO, USA). Antibodies were purchased from Abcam (RRID:SCR\_012931, anti- Iba-1; cat# ab5076), Promega (RRID:SCR\_006724; anti-  $\beta$ III-tubulin; cat# G7121) and Dako (RRID:SCR\_013530; anti- GFAP cat# Z0334). Fluorescent secondary antibodies were purchased from Jackson ImmunoResearch (RRID:SCR\_010488; West Grove, PA, USA). All antibodies were characterized and validated by the manufacturers.

**Synthesis and characterization of G5G2.5.** G5G2.5 tecto-dendrimers were synthesized and characterized as previously described (Schilrreff et al. 2012). Then, the tecto-dendrimer and the G6.5 dendrimer were labeled with FITC as described in (Kitchens *et al.* 2006) and (Schilrreff et al. 2012) with minor modifications. In brief, FITC (5 mg/mL) was dissolved in acetone and slowly added to G5G2.5 solutions at a 1:20 molar ratio, followed by incubation at room temperature for 24 hours in the dark. The FITC-labeled tectodendrimer was then separated from free FITC by size-exclusion chromatography on a Sephadex-G25 column.

The physicochemical characteristics of G5G2.5 tecto-dendrimer have been previously described in Schilrreff et al., (2012). In brief, the MW of G5G2.5 as estimated by MALDI-TOF-MS had a molecular weight peak at ~87,000 Da, with a MW distribution between 75,000 and 96,000 Da (Schilrreff et al. 2012). Regarding shape and size, TEM images showed fractal structured aggregates and spherical structures with an average diameter of  $7.20 \pm 2.06$  nm. The hydrodynamic diameter of G5G2.5 was around 11 nm both in HBSS and in culture media (MEM). On the other hand, the Z-potential of G5G2.5 in HBSS was slightly negative (-4 to -9 mV), while it decreased in culture media to -16.6 (Schilrreff et al. 2012). Considering that each G5G2.5 consists of a single G5 core dendrimer, a mean of 9–10 G2.5 dendrimer shell would be surrounding the

central core, which corresponds to a saturation level of 60%–67%. The extent of FITC conjugation was determined by measuring the absorbance of labeled polymers at 492 nm using a UV-visible spectrophotometer (UV-1603; Shimadzu, Kyoto, Japan). Number of moles of FITC conjugated per polymer was calculated using FITC calibration curve in Tris-HCl buffer. The quantification of the amount of FITC per polymer conjugate showed 22 FITC molecules per G5G2.5 molecule (Schilrreff et al. 2012).

**Primary Cultures.** Brain cortical mixed glial cultures containing astrocytes and microglia were done from neonatal (P3-P5) rat pups (Wistar strain) as described in (Villarreal et al. 2014). Neonatal Wistar rat pups were obtained from pregnant rats from the Animal Facility of the School of Pharmacy and Biochemistry, University of Buenos Aires. To obtain astrocytic-enriched cultures, cells from primary glial cultures were subjected to shaking at 180 RPM for 48 hours (h) at 37°C to detach microglia and oligodendrocytes and a subsequent treatment with 5-fluorouracyl [50 µg/ml] to inhibit mitotic microglia. Cultures obtained with this procedure showed more than 98% astrocytes with positive GFAP staining. Hippocampal mixed cultures were obtained as described in Lee and Parpura (Lee & Parpura 2012), with minor modifications (Angelo et al. 2014) and experimental procedures were done after 8-10 days in vitro (DIV). Meningeal cells were obtained by collecting cortical meninges from P3-P5 rat pups in Hank's Balanced Salt Solution (HBSS). Then, enzymatic digestion was performed with 0.25% trypsin, 0.2% collagenase, in HBSS for 30 min at 37°C. Following mechanical disaggregation in the presence of 25 U of DNase I, cells were washed and the cell suspension from 5 meninges was grown to confluence (7-10 days) in DMEM/F12, 10% FBS, 100 µg/ml penicillin/streptomycin in a 3.5 cm diameter plate, previously coated with poly-L-lysine. Co-cultures were prepared by adding a suspension of 15,000–30,000 meningeal cells to each well of confluent astrocytes prepared in a 24-well plate. Co-cultures were incubated in DMEM/F12, 10% FBS, 100 µg/ml penicillin/streptomycin for 2–3 days.

**Glial activation experiments.** Oxygen and glucose deprivation (OGD) exposure was performed by extracting the culture medium and replacing it with glucose- and serum-free DMEM and incubating the cells for 1 h in 0.1% O<sub>2</sub>, 5% CO<sub>2</sub> and balance N<sub>2</sub>. Glial exposure to LPS was done for 3 h. In all experiments, exposure to G5G2.5 was done after the indicated treatments, for 18 h at 37°C (as determined by the time course experiment, figure 1), unless stated otherwise. Cell

Accepted Article

fixation was done with 4% PFA- 4% sucrose PBS solution for 15 min at room temperature. For the lysosomal assay, LysoTracker was incubated for 15 min after exposure to the tecto-dendrimer. Cell viability upon treatment with the tecto-dendrimer was measured by the MTT assay following manufacturer instructions.

**Brain ischemia by cortical devascularization.** Adult male Wistar rats (300-350 g) were obtained from the Animal Facility of the School of Pharmacy and Biochemistry, University of Buenos Aires. Animals were housed in a controlled environment (12/12-h light/dark cycle, controlled humidity and temperature, free access to standard laboratory rat food and water) under the permanent supervision of a professional veterinarian. For all surgical procedures animals were anaesthetized with ketamine/xylazine (90/10 mg/kg i.p.). Rats were subjected to a unilateral cortical devascularization (CD) as previously described (Herrera & Robertson 1989, Villarreal *et al.* 2011, Villarreal *et al.* 2016) making every effort to reduce the suffering by applying an anesthetic mixture that has analgesic effects (Lee-Parritz, 2007) and the number of animals used was reduced by the appropriate calculations (see below) and by using the contralateral non ischemic hemisphere as internal control in each animal. Briefly, rats were placed in a stereotaxic frame so that the head was held in place during the procedure, and after dissecting the temporal muscle and the fascia, a small 2x2 mm surface of the skull between the coronal suture and the bregma line was removed, exposing the underlying vasculature. Using a 27-gauge needle, a small portion of the exposed pia was removed, disrupting pial blood vessels and generating a highly localized focal ischemic lesion. Immediately, small sterile cotton pieces were applied on the cortical surface to stop the bleeding (usually not longer than 50 seconds). Finally, the incision was closed, and the animals were monitored for complete recovery before returning them to their cages. After 3 days the tecto-dendrimer was delivered intracranially, close to the ischemic lesion (ipsilateral), and in the same coordinates of the contralateral hemisphere as a control. Briefly, rats were anaesthetized, placed in the stereotaxic frame, and a small hole was drilled into the skull. With a Hamilton syringe, 1  $\mu$ l of the G5G2.5-FITC [1mg/ml] was delivered both in the ipsilateral and contralateral (control) brain hemispheres. This volume was chosen to minimize damage associated with the injection (Murta *et al.* 2012, Murta *et al.* 2015), and the amount of tecto-dendrimer injected was in agreement with previous reports (Dai *et al.* 2010, Kang *et al.* 2010). The tecto-dendrimer was infused over a 5 minute period of time, with the needle left in place for an additional minute to minimize reflux. The injection was applied in the ipsilateral cortex, 1.5 mm away from the ischemic CD lesion, and in the contralateral hemisphere (bregma,

AP: - 2 mm; L:  $\pm$  3 mm; V: -1 mm)(Paxinos & Watson 1986). The incision was closed, and the animals allowed to recover as described above. After 24 h, animals were deeply anaesthetized with ketamine/xylazine (90/10 mg/kg, i.p.) and perfused through the left ventricle as described previously (Aviles-Reyes *et al.* 2010, Murta *et al.* 2015). Briefly, rats were perfused with heparinized saline followed by ice cold 4% paraformaldehyde in 0.1 M phosphate buffer (PB), pH 7.2. Brains were dissected and placed in the same fixative for 90 minutes at 4°C, followed by sequential cryoprotection in a 5-30% sucrose 0.1M PB solution. Finally, brains were snap frozen and 40  $\mu$ m serial coronal sections were cut in a cryostat. The animal care for this experimental protocol was in accordance with the NIH guidelines for the Care and Use of Laboratory Animals, the principles presented in the Guidelines for the Use of Animals in Neuroscience Research by the Society for Neuroscience, the ARRIVE guidelines, and was approved by the CICUAL committee of the School of Medicine, University of Buenos Aires (Res. 2873/15). No randomization was performed since all animals received tecto-dendrimer on the ipsilateral hemisphere and the contralateral hemisphere were used as internal control for non-ischemic hemisphere.

**Immunofluorescence.** Brain sections were simultaneously processed in the free floating state as previously described (Aviles-Reyes *et al.* 2010, Angelo *et al.* 2014). Isotypic specific secondary antibodies labeled with Alexa 488 or 594 were used, and counterstaining was made with DAPI 0.1  $\mu$ g/ml. For cell cultures, fixed cells were washed three times with cold phosphate-buffered saline (PBS) and permeabilized with 0.1% Triton X-100. The procedure was then followed as stated for tissue sections, using the indicated dilutions of the primary antibodies with the exception that Triton X-100 was included neither in the blocking nor in the antibody solution. Epifluorescence images were obtained in an Olympus IX-81 microscope equipped with a DP71 camera (Olympus, Tokyo, Japan). At least 25 randomly collected images were used for each treatment.

**Quantitative studies and statistical analysis.** Each *in vitro* experiment was repeated three times using duplicates or triplicates in each experiment. Analysis was made in blind conditions on coded images. Experiments involving animals were performed independently three times, and each experiment used at least three animals based in the past experience with the animal model (Villarreal *et al.*, 2014; 2016) and sample size calculations by resource equation (Charan and Kantharia, 2013). This calculation rendered a total number of 10 animals as necessary for these



Accepted Article

experiments since only one group was defined, with an unique dose and being the internal control the contralateral hemisphere in each animal. Representative experiments and photographs are presented in the figures. Data is expressed as mean  $\pm$  SEM. Data were analysed for normal distribution and homogeneity of variances and then subjected to the appropriate test (parametric or non-parametric) as stated in each figure legend. The statistical software package used was GraphPad Prism 5.0, (San Diego, CA) and statistical significance was assumed when  $p < 0.05$ . All detailed experimental protocols and antibody sources are available from authors under request.

## RESULTS

### **G5G2.5 tecto-dendrimer uptake by glial cells *in vitro*:**

In the first set of experiments we tested the ability of glial cells in glial mixed cultures, containing astrocytes, microglia and oligodendrocytes, to incorporate the FITC-labeled G5G2.5 tecto-dendrimer. As shown in figures 1A and 1B the G5G2.5 tecto-dendrimer was incorporated to glial cells in a dose-dependent manner. Unspecific uptake or adsorption was evaluated using free FITC in an equivalent molar concentration to that loaded in the tecto-dendrimer (Figure 1B). The kinetics of glial uptake was evaluated by incubating the FITC labeled G5G2.5 tecto-dendrimer during different periods of time and we found that uptake is time-dependent up to 6 h, and then incorporation reaches a plateau (Figure 1C-D). The G5G2.5 tecto-dendrimer showed improved uptake by glial cells when compared with a G6.5 dendrimer loaded with FITC (G6.5-FITC) as a control (Supplementary Figure 1). Specifically, the kinetics of glial uptake for the G6.5-FITC [0.1 $\mu$ M] revealed a much lower incorporation, with a plateau reached within the first hour of incubation (Supplementary figure 2). The G6.5-FITC was used as control since this dendrimer has a similar size and z potential to that measured for the G5G2.5 tecto-dendrimer (Schilrreff et al, 2012). We then analyzed the toxicity of the G5G2.5 tecto-dendrimer by incubating it during 18 h, and studied cell survival by measuring the mitochondrial activity using the MTT assay. As shown in figure 1E, a statistically significant loss of viability of glial cells was found at a tecto-dendrimer concentration of 1  $\mu$ M. Based on this result, for the subsequent experiments we set the dose at 0.1  $\mu$ M to prevent the cytotoxic effects of the tecto-dendrimer.

### **Cell specificity of the G5G2.5 tecto-dendrimer uptake by glial cells *in vitro*:**

Since glial cells *in vivo* largely outnumber the number of neurons, we then set a dissociated mixed cell culture from postnatal rat hippocampi (Lee & Parpura 2012, Angelo et al. 2014) that better resembles the situation in the intact CNS containing different neuronal phenotypes in addition to glial cells. We exposed these cultures to 0.05, 0.1 or 1  $\mu$ M FITC-labeled G5G2.5 tecto-dendrimer and observed an absence of neuronal uptake of the tecto-dendrimer at all tested concentrations (Figure 2A). In the mixed postnatal rat hippocampi cultures, we repeatedly observed microglia and astrocytes engulfing the FITC-labeled tecto-dendrimer (Figure 2B). Interestingly, exposure to oxygen and glucose deprivation (OGD), an *in vitro* condition that mimics the metabolic restriction produced by *in vivo* ischemia, dramatically increased tecto-dendrimer uptake by glial cells but did not produce tecto-dendrimer internalization in hippocampal neurons in mixed cultures (Figure 2B). Remarkably, the OGD-induced tecto-dendrimer incorporation seems to be a specific effect since it was not seen of the similar size G6.5-FITC dendrimer (Supplementary figure 1).

We next set up mixed glial cultures containing only astrocytes and microglia, incubated them with the FITC-labeled G5G2.5 tecto-dendrimer at a concentration of 0.1  $\mu$ M, and analyzed the comparative tecto-dendrimer uptake between microglia and astroglia. As shown in Figure 2C and 2D, microglia incorporated the FITC-labeled G5G2.5 tecto-dendrimer more efficiently, when compared with astrocytes, in control culture conditions without metabolic restrictions.

### **Reactive glia increases G5G2.5 tecto-dendrimer uptake:**

The previous result showing an increased ability of microglia to uptake the tecto-dendrimer is not surprising, since brain resident microglial cells are the professional macrophages in the CNS and they have a main role in innate immunity surveillance. Following CNS injury, in neurodegenerative diseases or even in sterile injury conditions, such as brain ischemia, both microglia and astroglia become activated and suffer a dramatic change in their physiological behavior. In addition, the ischemic core is rapidly invaded by blood-borne immune cells (reviewed in Benakis *et al.* 2014). After 2-4 weeks, reactive astrocytes reorient their processes into a dense mesh that forms a wall-like structure described as the glial scar, which was classically regarded as a main obstacle for axonal regrowth and neuronal reconnection (Burda & Sofroniew 2014).

In an attempt to reproduce *in vitro* the plethora of conditions faced by the different cell types, and in order to analyze the ability of the G5G2.5 tecto-dendrimer to reach each of these cell types, we set up different types of cultures exposed to oxygen and glucose deprivation (OGD), a paradigm that reproduces the metabolic features of the ischemic region. Firstly, we tested hippocampal neuro-glial mixed cultures and glial mixed cultures exposed to OGD. The results showed that OGD exposure globally increased the FITC-G5G2.5 uptake by glial cells both in hippocampal neuro-glial (Figure 2B) or mixed glial cultures (Figure 3A-B). LPS is a classical microglial and astroglial activator that engages the innate immunity receptor Toll-like 4 and facilitates the pro-inflammatory polarization (Liddel et al. 2017, Rosciszewski *et al.* 2017). As shown in Figure 3 (A-B) LPS exposure was not so efficient in stimulating the G5G2.5 uptake, thus demonstrating that the OGD-induced increase in tecto-dendrimer incorporation to glial cells is a specific effect. We then analyzed if OGD conditions facilitate the FITC labeled G5G2.5 uptake specifically in astrocytes. In figure 3C representative images and quantitative analysis of GFAP-labeled astrocytes in control and OGD conditions show that an increased number of GFAP+ astrocytes incorporated the FITC labeled G5G2.5 when exposed to OGD. On the other hand, studies performed on microglial cells present in those mixed cultures confirmed that OGD did not affect the microglial ability to uptake the tecto-dendrimer (Figure 3D). The comparative analysis of microglial and astroglial tecto-dendrimer uptake clearly showed that astrocytes reach the microglial ability to incorporate G5G2.5 tecto-dendrimer after OGD (Figure 3E). We conclude that OGD increases astroglial ability to engulf G5G2.5 tecto-dendrimer, but without affecting microglial G5G2.5 uptake.

Having demonstrated that astrocytes exposed to OGD *in vitro* increase tecto-dendrimer uptake, we next tested a paradigm that produces scar-like structures *in vitro* to study the tecto-dendrimer uptake by glial scar astrocytes. Glial scar formation is a key feature of focal CNS lesions, and it is considered the final step in astroglial activation following CNS injury (Sofroniew & Vinters 2010). As previously shown by Wanner and colleagues (Wanner *et al.* 2008, . 2013), primary astrocytes actively surround macrophages and spontaneously form scar-like structures that corral inflammatory meningeal macrophages in a STAT-3 dependent manner. In order to assess the tecto-dendrimer avidity in astrocytes with a different activation profile, we used a similar experimental paradigm (Wanner et al. 2008, 2013); we incubated primary astrocytes with meningeal cells, and allowed the formation of scar-like structures. Once the glial scar-like structures were formed (48-72 h), we exposed the cultures to 0.1  $\mu$ M FITC-labeled G5G2.5 tecto-dendrimer and observed that astrocytes incorporated the dendrimer, but without showing increased uptake by scar-forming astrocytes (Supplementary Fig. 2). These results corroborate

the differential response astrocytes have depending on the context, and show a preferential uptake of the G5G2.5 tecto-dendrimer by the early OGD activated astrocytes, and not by the glial-scar forming astrocytes.

#### **G5G2.5 tecto-dendrimer uptake by glial cells is an active process:**

Having shown that tecto-dendrimer uptake is preferentially done by astrocytes and microglia, and that OGD specifically increases astroglial, but not microglial uptake, we next studied the characteristics of the internalization process in glial cells and the subcellular localization of the dendrimer after uptake. We first determined that dendrimer uptake in the first hour of incubation dramatically decreased when culture temperature was reduced to 4°C (Figure 4A). The number of cells engulfing the G5G2.5-FITC tecto-dendrimer was lower (Figure 4B) but also the amount of nanoparticles effectively incorporated to cells seemed to be reduced, as shown in high magnification images (Figure 4C). The sub-cellular destination is a key feature to design the chemical interaction between the dendrimer and the potential cargo drug. After allowing the FITC-labeled G5G2.5 tecto-dendrimer to be incorporated for 18 h, we found that subcellular localization of the tecto-dendrimer colocalized with the lysosomal marker LysoTracker (Figure 4D). We conclude that G5G2.5 tecto-dendrimer is incorporated to glial cells by an active mechanism requiring metabolic activity and that nanoparticles reach the lysosomes.

#### **G5G2.5 tecto-dendrimer reaches glial cells in the ischemic brain**

Experimental models of focal ischemia in rodents reproduce most of the clinical features found in ischemic human brains. Unilateral cortical devascularization (CD) induces a permanent cortical focal ischemia with a clearly defined ischemic core and surrounding penumbra (Villarreal et al. 2014, 2016). At 3 days post ischemic lesion (DPL), the ischemic core presents a GFAP-negative staining, and is invaded by blood-borne macrophages cells, whereas the surrounding penumbral area shows hypertrophied GFAP+ reactive glia. We performed the CD focal ischemic lesion on male Wistar rats and 3 days later (3DPL) FITC-labeled G5G2.5 tecto-dendrimer was administered locally by intra-cortical injection, both in the ipsilateral and contralateral hemispheres, at 1.5 mm from the ischemic core. In figure 5A, low magnification images show the G5G2.5-FITC dendrimer uptake by cells in the ischemic lesion, while in the contralateral hemisphere the dendrimer remains in the injection site, but located in the extracellular space since no cell images were

observed in the hemisphere (Figure 5A). Detailed imaging showed that G5G2.5 tecto-dendrimer accumulates in the area of the lesion, and more specifically is taken up by cells within the core and penumbra. We then identified the cells that uptake the G5G2.5-FITC tecto-dendrimer. As shown in figure 5B, immunostaining studies evidenced that tecto-dendrimer is incorporated preferentially to microglia and macrophages infiltrating the ischemic core, that is essentially free of astrocytes at this time point after ischemia (3DPL). In the core, G5G2.5-FITC tecto-dendrimer colocalized with Iba-1 microglia/macrophage marker (Figure 5B, lower panel). While GFAP+ hypertrophied astrocytes localized in the penumbra were essentially free of G5G2.5-FITC tecto-dendrimer, some penumbral astrocytes in the demarcation zone near the core showed faint images of G5G2.5 uptake (Figure 5C). We conclude that most of the G5G2.5 tecto-dendrimer is incorporated to microglial cells and macrophages within the ischemic core, an area essentially free of GFAP+ astrocytes.

#### **DISCUSSION:**

The present study demonstrates the specific uptake of tecto-dendrimers by glial cells *in vitro* and *in vivo* in the ischemic brain. The tecto-dendrimer structure is composed of a shell consisting of G2.5 carboxyl-terminated PAMAM dendrimers and an amino G5 core dendrimer. The tecto-dendrimer structure was previously characterized as having a molecular weight similar to the G6.5 dendrimer, but showing a less-crowded surface (Schilrreff et al. 2012). The less crowded surface is an advantage at time of performing specific reactions with the loaded drug; otherwise it would show steric hindrance. In our case, the G2.5 carboxi-dendrimer shell covered the dendritic core formed by a G5-amino dendrimer, and the resulting tecto-dendrimer prevented the toxic effects of amino-surface dendrimers (Schilrreff et al. 2012).

The G5G2.5 tecto-dendrimer was specifically incorporated to microglia and astrocytes. *In vitro* dose-response and time-dependency studies have shown that this tecto-dendrimer has an interesting non-toxic concentration window, and that the uptake rapidly reaches a plateau, being highly specific to glial cells. The specific mechanisms involved in tecto-dendrimer internalization in glial cells are yet to be fully defined, but we here show that uptake is an active cellular process requiring metabolic activity and that the subcellular destination is the lysosomal pathway. In addition, the G5G2.5-FITC uptake is sensitive to inhibitors of the endocytic processes in a melanoma cell line (Schilrreff et al. 2014). Mammalian cells incorporate nanoparticles by endocytosis; this process can be classified as phagocytosis or pinocytosis (Sahay et al. 2010).

While immune professional cells such as microglia exploit their ability to do phagocytosis, astrocytes and other cell types usually perform pinocytosis. Microglial cells are the professional resident macrophages in the CNS and it should not be surprising that they engulf particulate materials such as dendrimeric nanoparticles in pathological settings (Kannan et al. 2012, Couturier *et al.* 2016). In fact, we show here that G5G2.5 tecto-dendrimer is incorporated to microglia *in vitro* and *in vivo*. On the other hand, astrocytes have not been classically regarded as cells specialized in the engulfment of particulate materials. However, a growing body of data is showing that astrocytes have the ability of engulfing synaptic components in physiological conditions (Risher *et al.* 2014), apoptotic bodies, extracellular Amyloid  $\beta$  and other cellular components including myelin debris (Kalmar *et al.* 2001, Loov *et al.* 2012, Cornejo & von Bernhardt 2013, Couturier et al. 2016, Ponath *et al.* 2016). The mechanisms by which astrocytes engulf synaptosomes and particles are not fully understood, but available data demonstrate that during development astrocytes cooperate with microglia engulfing synaptic components (Hong *et al.* 2016). On the other hand, phagocytosis under pathological conditions has been related to a bouquet of molecules and pathways including pattern recognition receptors such as RAGE and TLR and scavenger receptors (Villarreal et al. 2014, Loov et al. 2012, Cornejo & von Bernhardt 2013, Ponath et al. 2016). In addition, other authors have observed internalization of dendrimeric nanoparticles by astrocytes (Cerqueira et al., 2012, 2013;Salgado *et al.* 2010). Our results are in accordance with these data and provide support to idea that astrocytes, and particularly reactive astrocytes, are capable of phagocytizing molecules, and specifically nanoparticles resembling the ability previously regarded for innate immunity responses by professional immune cells.

Reactive gliosis is a generic response of glial cells upon brain injury. Following acute or chronic injury, microglia and astrocytes become reactive, and enter into a gene expression program that changes dramatically their physiological role. Importantly, the reactive microglial and astroglial conversion to the pro-inflammatory M1 and A1 phenotypes is highly detrimental for neuronal survival (Liddelow et al. 2017). Reactive astrocytes seem to increase their ability to incorporate nanoparticles, as shown for hydroxyl-G4 labeled dendrimers in a model of maternal inflammation-induced cerebral palsy in rabbits (Kannan et al. 2012, Dai *et al.* 2010); while reducing their ability to engulf synaptic components and myelin debris *in vitro* (Liddelow et al. 2017). Our results consistently showed that microglial cells preferentially incorporate the tecto-dendrimer in control culture conditions; however reactive astrocytes significantly increased their ability to uptake the G5G2.5 tecto-dendrimer when exposed to OGD. *In vivo*, following intracortical injection, the G5G2.5 tecto-dendrimer uptake was observed specifically in the ischemic hemisphere. After ischemia by cortical devascularization (Villarreal et al. 2014, Herrera

& Robertson 1989, Villarreal et al. 2016), the G5G2.5 uptake was detected in the ipsilateral hemisphere, specifically in the core and demarcation zone of the penumbra. The majority of cells incorporating the G5G2.5 tecto-dendrimer were identified as Iba-1+ microglia and macrophages. This was not an unexpected finding, since the resident microglia and blood-derived macrophages are the professional cells involved in debris and particle clearing. Surprisingly, only a few pale images of GFAP+ astrocytes incorporating G5G2.5 tecto-dendrimer were observed in the penumbral demarcation zone. Different explanations can be hypothesized for this effect; ranging from a simply quenching of the nanoparticle due to the uptake by professional macrophages and activated microglia, to a more complex situation where astroglial heterogeneity, exacerbated by the ischemic injury, defines different types of astrocytes, some of which can be more active in engulfing the dendrimer (Villarreal et al. 2016, Ramos 2016). Despite the fact that brain ischemia and other pathological states produce the BBB disruption, an obvious limitation of our *in vivo* approach is that intracortical administration overcomes the BBB limitation to access to the CNS. Further detailed pharmacokinetics studies will be required to analyze the detailed biodistribution of the tecto-dendrimer.

The targeted drug delivery to glial cell specific phenotypes could prevent their conversion to the detrimental phenotypes and/or preserve the beneficial ones. In terms of therapy, the intrinsic ability of the G5G2.5 tecto-dendrimer to specifically localize to reactive astrocytes and microglia activated by ischemia or *in vitro* OGD can enable targeted delivery of molecules to these specific cell types. In this respect, G5G2.5 tecto-dendrimer shows a similar ability to that observed for G4-OH dendrimer in several recent reports (Dai et al. 2010, Kannan et al. 2012, Zhang *et al.* 2016). In general terms, the cell specificity observed for different dendrimers seems to depend on the surface chemistry and the contextual inflammatory environment (Barata *et al.* 2011, Kim *et al.* 2010, Albertazzi *et al.* 2010, Lesniak et al. 2013, Zhang et al. 2016); in line with this, in our experiments the G5G2.5 tecto-dendrimer showed increased uptake in ischemia-related neuroinflammation. Interestingly, astroglial uptake of the dendrimer is also increased in OGD conditions *in vitro*, even when astrocytes were devoid of other cell types. This result implies that reactive astrocytes induced by OGD have the intrinsic ability to engulf the tecto-dendrimer, without requiring secondary signals from other cell types.

In general terms, tecto-dendrimers show many advantages over classical dendrimers, including the high loading capacity and less crowded surface compared with the native dendrimers of similar molecular weight, the possibility of having differential superficial domains and inner structure to improve the molecular interaction with the loaded compound and to provide better

cell selectivity, and the relatively easier synthesis compared with the classical divergent or convergent methods for high generation dendrimer synthesis (Schilrreff et al. 2012, Hawker & Fréchet 1990). The present findings expand the repertory of available dendrimers that can be used for specific glial-targeted therapies in different CNS pathological states and diseases where neuroinflammation drives secondary neuronal death. In addition, tecto-dendrimers can be also suitable for the glial-cell specific delivery of molecules, expression genes, or gene expression modifiers in experimental settings.

We conclude that G5G2.5 tecto-dendrimer has a potential use as carrier molecule for glial-cell based therapy, a yet unexplored strategy to control or prevent reactive glia polarization to the pro-inflammatory neurodegenerative phenotype. This approach would bring the opportunity of reducing neuroinflammation to mitigate secondary neuronal death, thus improving patient recovery in stroke and other devastating diseases of the CNS.

Involves human subjects:

If yes: Informed consent & ethics approval achieved:

=> if yes, please ensure that the info "Informed consent was achieved for all subjects, and the experiments were approved by the local ethics committee." is included in the Methods.

ARRIVE guidelines have been followed:

Yes

=> if No or if it is a Review or Editorial, skip complete sentence => if Yes, insert "All experiments were conducted in compliance with the ARRIVE guidelines." unless it is a Review or Editorial

Conflicts of interest: none

=> if 'none', insert "The authors have no conflict of interest to declare."

=> otherwise insert info unless it is already included



=> if yes, please see Comments from the Journal for further information => if no, no information need to be included in the manuscript

### Acknowledgements:

Supported by grants CONICET PIP 387 (to AJR), ANPCYT PICT2012-1424/PICT2015-1451 (to AJR), UBACYT (to AJR). VM, PS, MJM and AJR are researchers from CONICET (Argentina). GR is a doctoral fellow from CONICET. We thank Biot. Andrea Pecile and Manuel Ponce for the animal care. The authors declare that there are no conflicts of interest.

### Figure Legends

**Figure 1. Dose-response and temporal dynamics of G5G2.5 uptake. (A)** Mixed glial primary cultures incubated with different concentrations of G5G2.5-FITC, or with free FITC for 18 hours. **(B)** Quantitative study showing the tecto-dendrimer uptake as the concentration increases; high FITC concentration is the molar equivalent of the relative FITC concentration in the 1  $\mu$ M G5G2.5-FITC, and low FITC concentration is equivalent to that one found in the 0.1  $\mu$ M G5G2.5. N=3 (independent experiments, with triplicates in each); One way ANOVA; Bonferroni's Multiple Comparison Test. **(C)** Time-course of tecto-dendrimer uptake by glial cells shows that the incorporation increases with time; concentration tested is 0.1  $\mu$ M G5G2.5-FITC. **(D)** Quantitative evaluation of tecto-dendrimer uptake showing that dendrimer is internalized as early as 0.5 hours, and its incorporation continues to increase, reaching a plateau at 6 hours. N=3 (independent experiments, with triplicates in each); One way ANOVA; Bonferroni's Multiple Comparison Test. **(E)** Cell viability studied with the MTT assay to determine the impact of tecto-dendrimer in primary glia viability. N=3 (independent experiments, with duplicates in each); One way ANOVA; Dunnett's Multiple Comparison Test. \*  $p < 0.05$ ; \*\*  $p < 0.01$ ; \*\*\*  $p < 0.001$ . Scale bars = 50  $\mu$ m.

**Figure 2. Cell specificity in the G5G2.5 tecto-dendrimer uptake. (A)** The incubation of the FITC-labeled G5G2.5 tecto-dendrimer [0.1  $\mu$ M] for 18 h in primary mixed neuro-glial hippocampal cultures shows that the G5G2.5 is not incorporated into  $\beta$ III-tubulin+ neurons (red) but clearly engulfed by glial cells (arrows). **(B).** Specific immunostaining for GFAP astroglial marker (red) in primary mixed neuro-glial hippocampal cultures showed that astrocytes and microglia are the

cells that preferentially uptake the FITC-G5G2.5 tecto-dendrimer. OGD exposure for 1 h dramatically increased glial uptake of the FITC-labeled G5G2.5 tecto-dendrimer, without evidence of neuronal uptake in these mixed neuro-glial hippocampal cultures. **(C)** Primary glial cultures exposed to 0.1  $\mu$ M FITC tecto-dendrimer for 18 hours show that both Iba-1+ microglia (red, upper panel), and GFAP+ astrocytes (red, lower panel) incorporate the FITC-G5G2.5 tecto-dendrimer. **(D)** Quantitative analysis of these cultures containing astrocytes and microglia showed that microglial cells are more capable to engulfing the G5G2.5-FITC tecto-dendrimer than astrocytes. N=3 (independent experiments, with triplicates in each); Unpaired t Test. \*  $p < 0.05$ . Bar = 100  $\mu$ m.

**Figure 3. Glial activation increases tecto-dendrimer incorporation.** **(A)** Representative images of primary mixed glial cell cultures exposed to activating stimuli (1 h of OGD, or 3 h of LPS), and then incubated with 0.1  $\mu$ M G5G2.5-FITC for 18 hours. **(B)** Higher magnification images of a similar experiment to that depicted in (A) showing that more cells incorporated the nanoparticle when exposed to either OGD or LPS. Quantification confirmed a significant increase in the G5G2.5-FITC uptake when the cells were exposed to OGD *in vitro*. N=3 (independent experiments, with triplicates in each); One way ANOVA. \*  $p < 0.05$ . **(C)** Representative images of GFAP+ astrocytes (red) showing G5G2.5-FITC (green) uptake in control and OGD conditions. Quantitative analysis showed that OGD exposure induced a significant increase of the tecto-dendrimer uptake in GFAP+ astrocytes. Unpaired t Test. \*  $p < 0.05$ . **(D)** Representative images of Iba-1+ microglia (red) showing G5G2.5-FITC (green) uptake in control and OGD conditions. Quantitative analysis showed that OGD exposure did not change tecto-dendrimer uptake in Iba-1+ microglia. N=3 (independent experiments, with triplicates in each); Unpaired t Test. \*  $p < 0.05$ . Scale bar = 100  $\mu$ m. **(E)** Comparative analysis of the ratio of microglia Iba-1+ vs. astrocytes GFAP+ engulfing the tecto-dendrimer in control and OGD conditions. Note that GFAP+ astrocytes increased the uptake in OGD. Unpaired t Test. \*  $p < 0.05$ . N=3 (independent experiments, with triplicates in each)

**Figure 4. Mechanisms of G5G2.5 incorporation and subcellular localization.** **(A)** Representative images of G5G2.5-FITC tecto-dendrimer incorporated to glial cells after 1 hour incubation at 4 or 37°C in mixed glial primary culture. Scale bars = 50  $\mu$ m **(B)** Quantification of the incorporation of the G5G2.5-FITC tecto-dendrimer, (N=3; independent experiments, with triplicates in each) analyzed by Mann-Whitney test, \*  $p < 0.05$ . Incubation at 4°C decreased the uptake of the

dendrimer. **(C)** Detailed microphotograph of live imaged unfixed cells incubated at 37°C or 4°C with G5G2.5-FITC tecto-dendrimer. Scale bar = 5  $\mu\text{m}$  **(D)** Representative images of primary mixed glial cultures exposed 1 hour to OGD, 18 hours to the tecto-dendrimer, and 15 minutes to lysosomal marker LysoTracker (LYSO) showing that G5G2.5 is incorporated to the lysosomes. Scale bars = 50  $\mu\text{m}$  and 5  $\mu\text{m}$ .

**Figure 5. Increased uptake of tecto-dendrimer after *in vivo* brain ischemia.** **(A)** Representative images of the ischemic lesion (ipsilateral) and contralateral hemisphere in rats subjected to focal brain ischemia. After 3 days post-ischemia, rats received 1 $\mu\text{l}$  of 12  $\mu\text{M}$  G5G2.5-FITC bilaterally, 1.5 mm apart from the focal ischemic site (yellow arrow indicates injection site) and images were obtained 24 h later. G5G2.5-FITC showed punctated staining indicative of cellular uptake in the ischemic core and penumbral demarcation zone. Contralateral hemisphere showed homogeneous fluorescence, indicative of the extracellular location of G5G2.5-FITC that was not incorporated to cells. Scale bar = 1 mm (upper panel); 100  $\mu\text{m}$  (lower panel). **(B)** Representative images of double staining with GFAP (astroglial marker) and Iba-1 (microglia/macrophage marker) showing that G5G2.5-FITC tecto-dendrimer was preferentially incorporated to microglia and macrophages in the core and penumbral demarcation zone. Ischemic core shows absence of GFAP-immunostained astrocytes and it is depicted with an asterisk (\*). Scale bar: 100  $\mu\text{m}$  (left panel); 25  $\mu\text{m}$  (right panel). **(C)** High magnification images of GFAP+ astrocytes in the penumbral demarcation zone showing a less intense G5G2.5-FITC incorporation compared with microglia and macrophages. N=3 (independent experiments, with triplicates in each).

## REFERENCES

- Albertazzi, L., Gherardini, L., Brondi, M., Sulis Sato, S., Bifone, A., Pizzorusso, T., Ratto, G. M. and Bardi, G. (2013) In vivo distribution and toxicity of PAMAM dendrimers in the central nervous system depend on their surface chemistry. *Mol Pharm*, **10**, 249-260.
- Albertazzi, L., Serresi, M., Albanese, A. and Beltram, F. (2010) Dendrimer internalization and intracellular trafficking in living cells. *Mol Pharm*, **7**, 680-688.
- Anderson, M. A., Ao, Y. and Sofroniew, M. V. (2014) Heterogeneity of reactive astrocytes. *Neurosci Lett*, **565**, 23-29.

Angelo, M. F., Aguirre, A., Aviles Reyes, R. X. et al. (2014) The proinflammatory RAGE/NF-kappaB pathway is involved in neuronal damage and reactive gliosis in a model of sleep apnea by intermittent hypoxia. *PLoS One*, **9**, e107901.

Aviles-Reyes, R. X., Angelo, M. F., Villarreal, A., Rios, H., Lazarowski, A. and Ramos, A. J. (2010) Intermittent hypoxia during sleep induces reactive gliosis and limited neuronal death in rats: implications for sleep apnea. *J Neurochem*, **112**, 854-869.

Barata, T., Teo, I., Lalwani, S., Simanek, E., Zloh, M. and Shaunak, S. (2011) Computational design principles for bioactive dendrimer based constructs as antagonists of the TLR4-MD-2-LPS complex. *Biomaterials*, **32**, 8702-8711.

Benakis, C., Garcia-Bonilla, L., Iadecola, C. and Anrather, J. (2014) The role of microglia and myeloid immune cells in acute cerebral ischemia. *Front Cell Neurosci*, **8**, 461.

Burda, J. E. and Sofroniew, M. V. (2014) Reactive gliosis and the multicellular response to CNS damage and disease. *Neuron*, **81**, 229-248.

Cerqueira, S. R., Silva, B. L., Oliveira, J. M., Mano, J. F., Sousa, N., Salgado, A. J. and Reis, R. L. (2012) Multifunctionalized CMChT/PAMAM dendrimer nanoparticles modulate the cellular uptake by astrocytes and oligodendrocytes in primary cultures of glial cells. *Macromol Biosci*, **12**, 591-597.

Cerqueira SR, Oliveira JM, Silva NA, Leite-Almeida H, Ribeiro-Samy S, Almeida A, Mano JF, Sousa N, Salgado AJ, Reis RL. Microglia response and in vivo therapeutic potential of methylprednisolone-loaded dendrimer nanoparticles in spinal cord injury. *Small*. 2013 Mar 11;9(5):738-49. doi: 10.1002/smll.201201888. Epub 2012 Nov 15. Erratum in: *Small*. 2016 Feb;12(8):972.

Charan J, Kantharia ND. How to calculate sample size in animal studies? *J.Pharmacol Pharmacother*. 2013 Oct;4(4):303-6. doi: 10.4103/0976-500X.119726.

Cornejo, F. and von Bernhardi, R. (2013) Role of scavenger receptors in glia-mediated neuroinflammatory response associated with Alzheimer's disease. *Mediators Inflamm*, **2013**, 895651.

Couturier, J., Stancu, I. C., Schakman, O., Pierrot, N., Huaux, F., Kienlen-Campard, P., Dewachter, I. and Octave, J. N. (2016) Activation of phagocytic activity in astrocytes by reduced expression of the inflammasome component ASC and its implication in a mouse model of Alzheimer disease. *J Neuroinflammation*, **13**, 20.

Dai, H., Navath, R. S., Balakrishnan, B., Guru, B. R., Mishra, M. K., Romero, R., Kannan, R. M. and Kannan, S. (2010) Intrinsic targeting of inflammatory cells in the brain by polyamidoamine dendrimers upon subarachnoid administration. *Nanomedicine (Lond)*, **5**, 1317-1329.

Grotta, J. C. and Hacke, W. (2015) Stroke Neurologist's Perspective on the New Endovascular Trials. *Stroke*, **46**, 1447-1452.

- Guo, Y., Zhao, Y., Wang, T., Li, R., Han, M., Dong, Z., Zhu, C. and Wang, X. (2016) Hydroxycamptothecin Nanorods Prepared by Fluorescently Labeled Oligoethylene Glycols (OEG) Codendrimer: Antitumor Efficacy in Vitro and in Vivo. *Bioconjug Chem*.
- Guo Y, Johnson MA, Mehrabian Z, Mishra MK, Kannan R, Miller NR, et al. (2016) Dendrimers Target the Ischemic Lesion in Rodent and Primate Models of Nonarteritic Anterior Ischemic Optic Neuropathy. *PLoS ONE* 11(4): e0154437. doi:10.1371/journal.pone.0154437
- Hawker, C. and Fréchet, J. (1990) Preparation of polymers with controlled molecular architecture. A new convergent approach to dendritic macromolecules. *J Am Chem Soc*, 7638–7647.
- Herrera, D. G. and Robertson, H. A. (1989) Unilateral induction of c-fos protein in cortex following cortical devascularization. *Brain Res*, **503**, 205-213.
- Hong, S., Dissing-Olesen, L. and Stevens, B. (2016) New insights on the role of microglia in synaptic pruning in health and disease. *Curr Opin Neurobiol*, **36**, 128-134.
- Huang, Y. C. and Feng, Z. P. (2013) The good and bad of microglia/macrophages: new hope in stroke therapeutics. *Acta Pharmacol Sin*, **34**, 6-7.
- Kalmar, B., Kittel, A., Lemmens, R., Kornyei, Z. and Madarasz, E. (2001) Cultured astrocytes react to LPS with increased cyclooxygenase activity and phagocytosis. *Neurochem Int*, **38**, 453-461.
- Kang, C., Yuan, X., Li, F., Pu, P., Yu, S., Shen, C., Zhang, Z. and Zhang, Y. (2010) Evaluation of folate-PAMAM for the delivery of antisense oligonucleotides to rat C6 glioma cells in vitro and in vivo. *J Biomed Mater Res A*, **93**, 585-594.
- Kannan, R. M., Nance, E., Kannan, S. and Tomalia, D. A. (2014) Emerging concepts in dendrimer-based nanomedicine: from design principles to clinical applications. *J Intern Med*, **276**, 579-617.
- Kannan, S., Dai, H., Navath, R. S., Balakrishnan, B., Jyoti, A., Janisse, J., Romero, R. and Kannan, R. M. (2012) Dendrimer-based postnatal therapy for neuroinflammation and cerebral palsy in a rabbit model. *Sci Transl Med*, **4**, 130ra146.
- Kim, I. D., Lim, C. M., Kim, J. B., Nam, H. Y., Nam, K., Kim, S. W., Park, J. S. and Lee, J. K. (2010) Neuroprotection by biodegradable PAMAM ester (e-PAM-R)-mediated HMGB1 siRNA delivery in primary cortical cultures and in the postischemic brain. *J Control Release*, **142**, 422-430.
- Kitchens, K. M., Kolhatkar, R. B., Swaan, P. W., Eddington, N. D. and Ghandehari, H. (2006) Transport of poly(amidoamine) dendrimers across Caco-2 cell monolayers: Influence of size, charge and fluorescent labeling. *Pharm Res*, **23**, 2818-2826.
- Lee-Parritz, D. Analgesia for rodent experimental surgery. *Israel Journal of Veterinary. Medicine*, v. 62, n.3-4, 2007.

- LeComte, M. D., Shimada, I. S., Sherwin, C. and Spees, J. L. (2015) Notch1-STAT3-ETBR signaling axis controls reactive astrocyte proliferation after brain injury. *Proc Natl Acad Sci U S A*, **112**, 8726-8731.
- Lee, W. and Parpura, V. (2012) Dissociated cell culture for testing effects of carbon nanotubes on neuronal growth. *Methods Mol Biol*, **846**, 261-276.
- Lesniak, W. G., Mishra, M. K., Jyoti, A., Balakrishnan, B., Zhang, F., Nance, E., Romero, R., Kannan, S. and Kannan, R. M. (2013) Biodistribution of fluorescently labeled PAMAM dendrimers in neonatal rabbits: effect of neuroinflammation. *Mol Pharm*, **10**, 4560-4571.
- Levine, D. A., Morgenstern, L. B., Langa, K. M., Skolarus, L. E., Smith, M. A. and Lisabeth, L. D. (2013) Does socioeconomic status or acculturation modify the association between ethnicity and hypertension treatment before stroke? *Stroke*, **44**, 3243-3245.
- Liddel, S. A., Guttenplan, K. A., Clarke, L. E. et al. (2017) Neurotoxic reactive astrocytes are induced by activated microglia. *Nature*.
- Loov, C., Hillered, L., Ebendal, T. and Erlandsson, A. (2012) Engulfing astrocytes protect neurons from contact-induced apoptosis following injury. *PLoS One*, **7**, e33090.
- Lothian-Tomalia, M. K., Hedstrand, D. M., Tomalia, D. A., Padias, A. B. and Jr., H. K. H. (1997) A contemporary survey of covalent connectivity and complexity. The divergent synthesis of poly(thioether) dendrimers. Amplified, genealogically directed synthesis leading to the dense packed state. *Tetrahedron*, **53**, 15495–15513.
- Murta, V., Farias, M. I., Pitossi, F. J. and Ferrari, C. C. (2015) Chronic systemic IL-1beta exacerbates central neuroinflammation independently of the blood-brain barrier integrity. *J Neuroimmunol*, **278**, 30-43.
- Murta, V., Pitossi, F. J. and Ferrari, C. C. (2012) CNS response to a second pro-inflammatory event depends on whether the primary demyelinating lesion is active or resolved. *Brain Behav Immun*, **26**, 1102-1115.
- Nance, E., Porambo, M., Zhang, F. et al. (2015) Systemic dendrimer-drug treatment of ischemia-induced neonatal white matter injury. *J Control Release*, **214**, 112-120.
- Paxinos, G. and Watson, C. (1986) The rat brain in stereotaxic coordinates. Academic Press, Orlando.
- Ponath, G., Ramanan, S., Mubarak, M., Housley, W., Lee, S., Sahinkaya, F. R., Vortmeyer, A., Raine, C. S. and Pitt, D. (2016) Myelin phagocytosis by astrocytes after myelin damage promotes lesion pathology. *Brain*.
- Ramos, A. J. (2016) Astroglial heterogeneity: merely a neurobiological question? Or an opportunity for neuroprotection and regeneration after brain injury? *Neural Regen Res*, **11**, 1739-1741.
- Risher, W. C., Patel, S., Kim, I. H. et al. (2014) Astrocytes refine cortical connectivity at dendritic spines. *Elife*, **3**.

- Rosciszewski, G., Cadena, V., Veronica Murta, P. D., Lukin, J., Alejandro Villarreal, P., Thierry Roger, P. and Alberto Javier Ramos, P. D. (Accepted with minor corrections) "Toll-like receptor 4 (TLR4) and triggering receptor expressed on myeloid cells-2 (TREM-2) activation balance astrocyte polarization into a proinflammatory phenotype". *Molecular Neurobiology*.
- Sahay, G., Alakhova, D. Y. and Kabanov, A. V. (2010) Endocytosis of nanomedicines. *J Control Release*, **145**, 182-195.
- Salgado, A. J., Oliveira, J. M., Pirraco, R. P. et al. (2010) Carboxymethylchitosan/poly(amidoamine) dendrimer nanoparticles in central nervous systems-regenerative medicine: effects on neuron/glial cell viability and internalization efficiency. *Macromol Biosci*, **10**, 1130-1140.
- Schilrreff, P., Cervini, G., Romero, E. L. and Morilla, M. J. (2014) Enhanced antimelanoma activity of methotrexate and zoledronic acid within polymeric sandwiches. *Colloids Surf B Biointerfaces*, **122**, 19-29.
- Schilrreff, P., Mundina-Weilenmann, C., Romero, E. L. and Morilla, M. J. (2012) Selective cytotoxicity of PAMAM G5 core--PAMAM G2.5 shell tecto-dendrimers on melanoma cells. *Int J Nanomedicine*, **7**, 4121-4133.
- Sofroniew, M. V. and Vinters, H. V. (2010) Astrocytes: biology and pathology. *Acta Neuropathol*, **119**, 7-35.
- Uppuluri, S., Swanson, D. R., Piehler, L. T., Li, J., Hagnauer, G. L. and Tomalia, D. A. (2000) Core-Shell Tecto(dendrimers): I. Synthesis and Characterization of Saturated Shell Models. *Advanced Materials*, **12**, 796-800.
- Villarreal, A., Aviles Reyes, R. X., Angelo, M. F., Reines, A. G. and Ramos, A. J. (2011) S100B alters neuronal survival and dendrite extension via RAGE-mediated NF-kappaB signaling. *J Neurochem*, **117**, 321-332.
- Villarreal, A., Rosciszewski, G., Murta, V., Cadena, V., Usach, V., Dodes-Traian, M. M., Setton-Avruj, P., Barbeito, L. H. and Ramos, A. J. (2016) Isolation and Characterization of Ischemia-Derived Astrocytes (IDAs) with Ability to Transactivate Quiescent Astrocytes. *Front Cell Neurosci*, **10**, 139.
- Villarreal, A., Seoane, R., Gonzalez Torres, A., Rosciszewski, G., Angelo, M. F., Rossi, A., Barker, P. A. and Ramos, A. J. (2014) S100B protein activates a RAGE-dependent autocrine loop in astrocytes: implications for its role in the propagation of reactive gliosis. *J Neurochem*.
- Wanner, I. B., Anderson, M. A., Song, B., Levine, J., Fernandez, A., Gray-Thompson, Z., Ao, Y. and Sofroniew, M. V. (2013) Glial scar borders are formed by newly proliferated, elongated astrocytes that interact to corral inflammatory and fibrotic cells via STAT3-dependent mechanisms after spinal cord injury. *J Neurosci*, **33**, 12870-12886.
- Wanner, I. B., Deik, A., Torres, M., Rosendahl, A., Neary, J. T., Lemmon, V. P. and Bixby, J. L. (2008) A new in vitro model of the glial scar inhibits axon growth. *Glia*, **56**, 1691-1709.

Zamanian, J. L., Xu, L., Foo, L. C., Nouri, N., Zhou, L., Giffard, R. G. and Barres, B. A. (2012) Genomic analysis of reactive astrogliosis. *J Neurosci*, **32**, 6391-6410.

Zhang, F., Nance, E., Alnasser, Y., Kannan, R. and Kannan, S. (2016) Microglial migration and interactions with dendrimer nanoparticles are altered in the presence of neuroinflammation. *J Neuroinflammation*, **13**, 65.



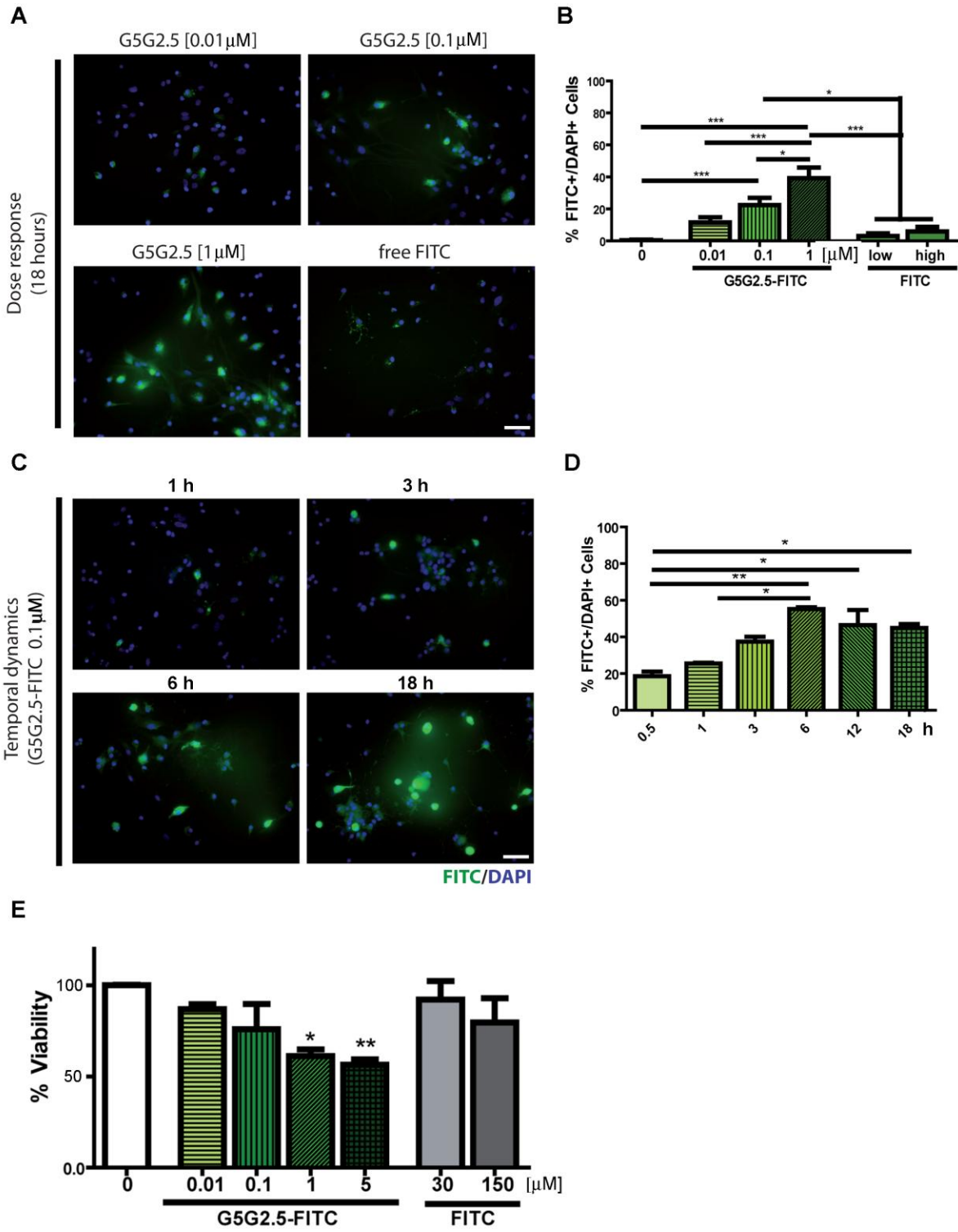


Figure 1

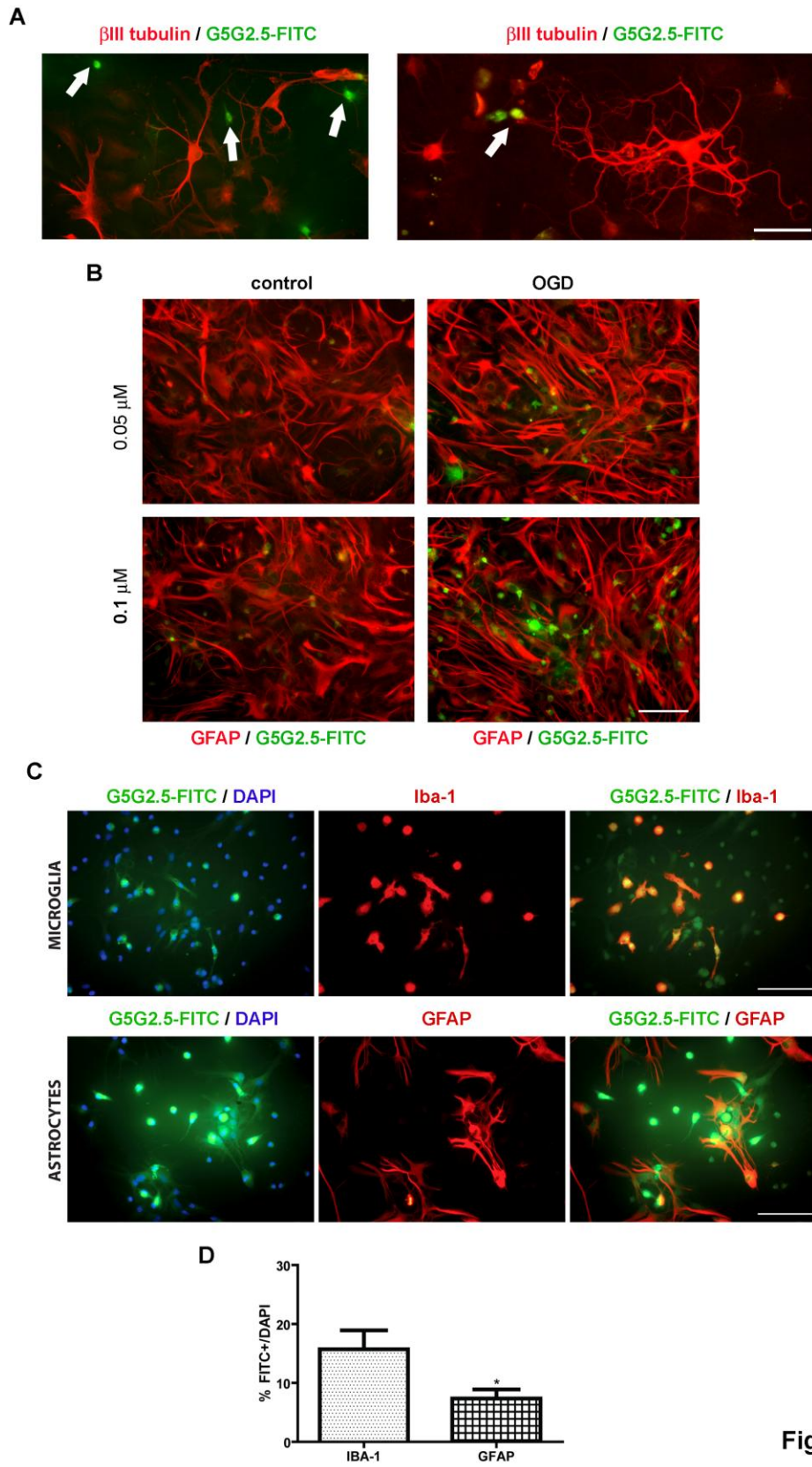


Figure 2

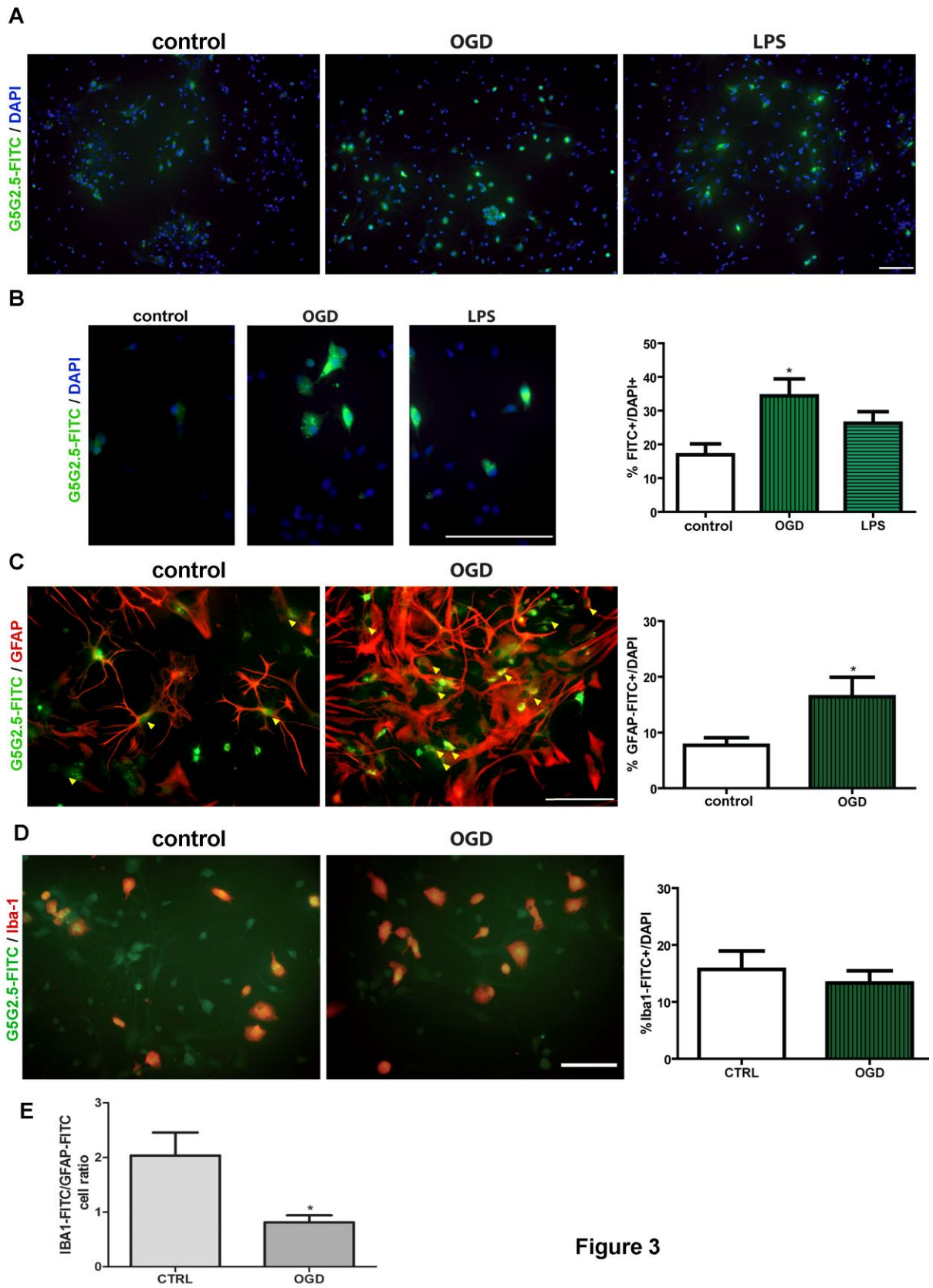
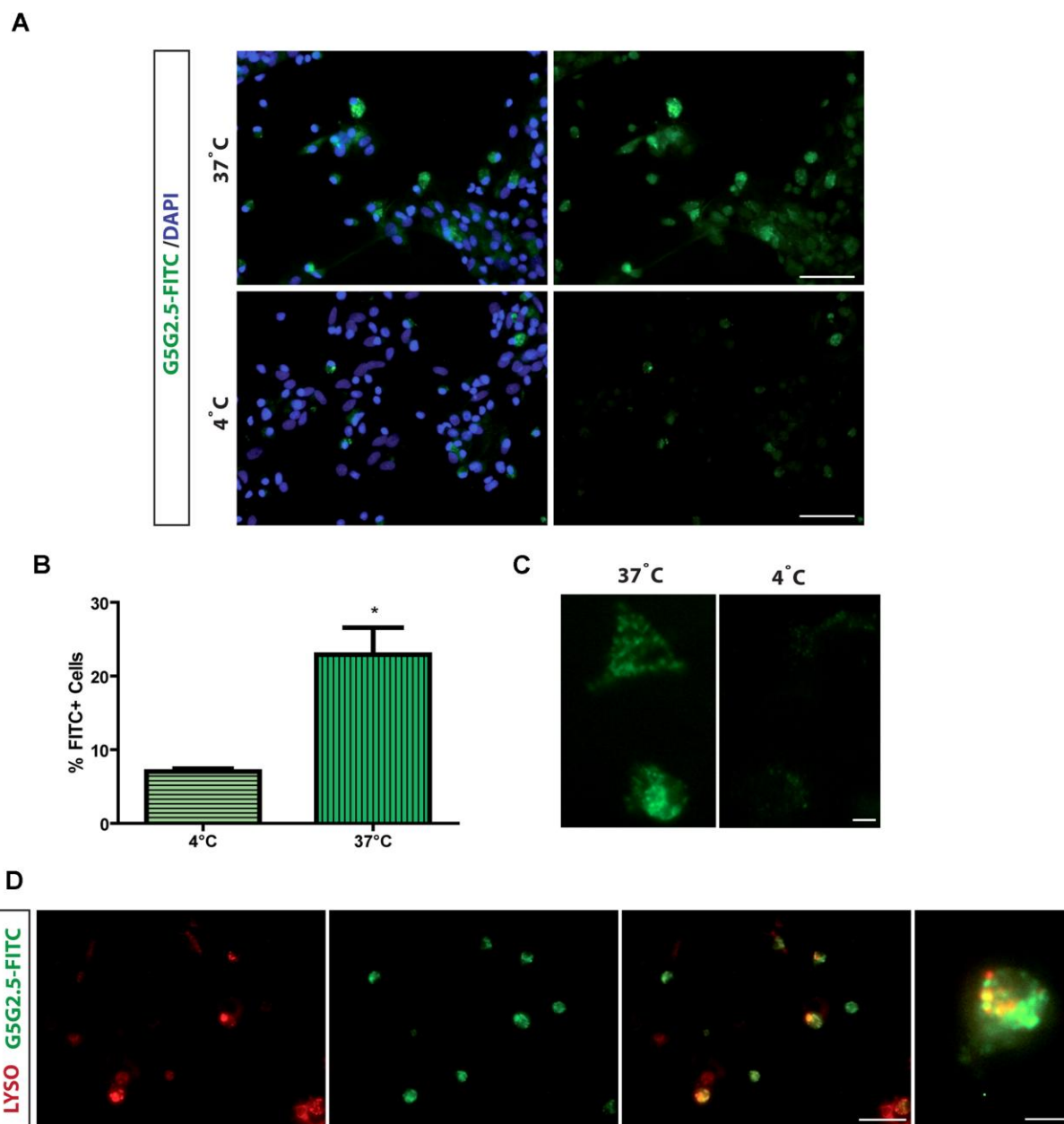


Figure 3





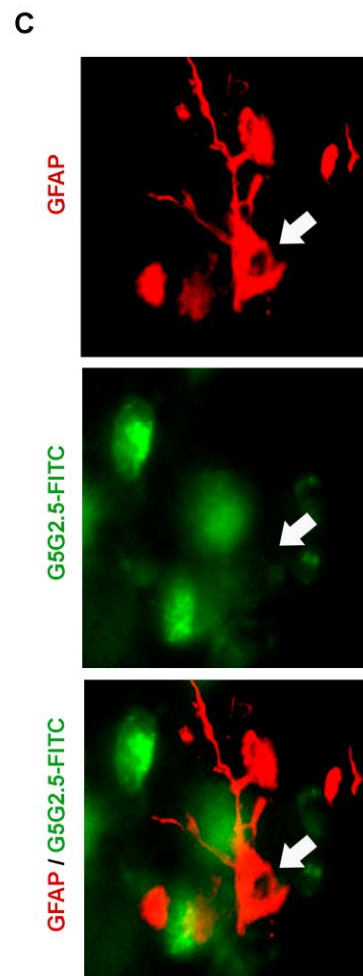
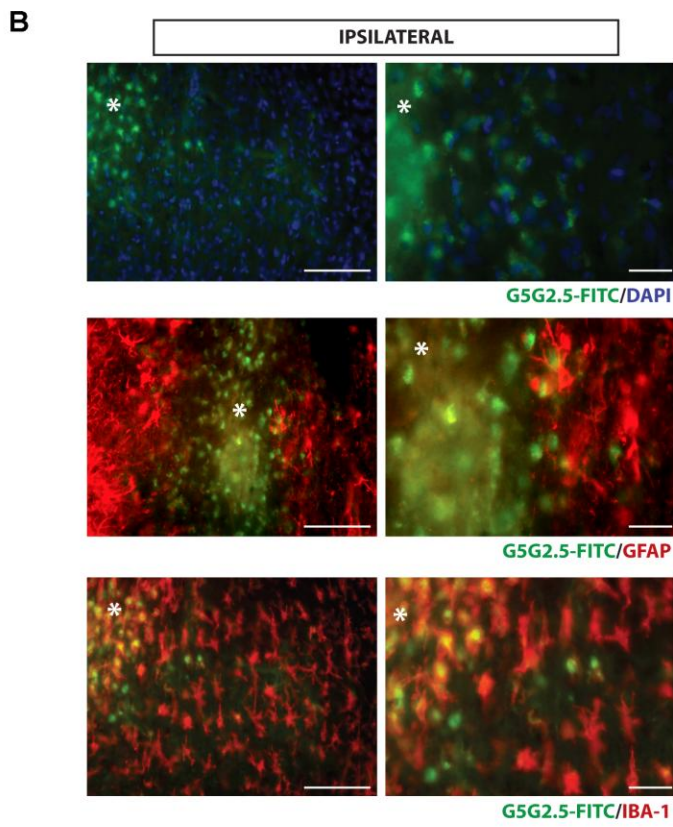
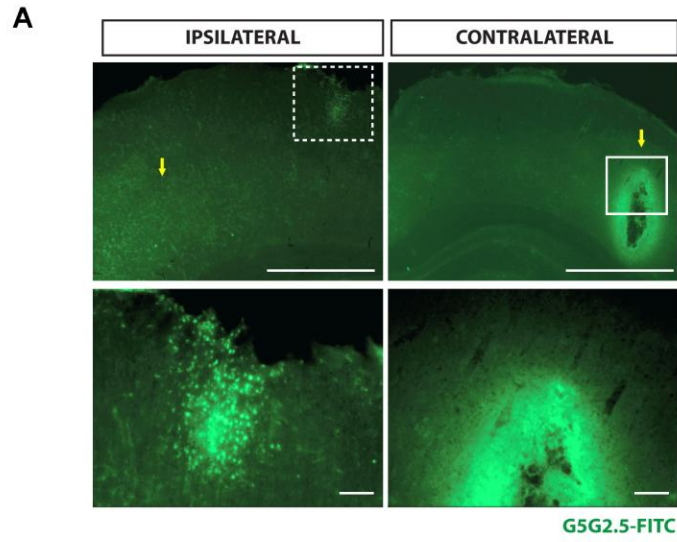


Figure 5